School of Computer Science, Engineering and Mathematics

Project:

THE RELATIONSHIP BETWEEN FEMUR MECHANICS AND MOVEMENT

by

Raissa Katembwe

Supervised by

Dr. Saulo Martelli

NOVEMBER 14, 2016

DECLARATION

'I certify that this thesis does not incorporate without acknowledgment any material previously submitted for a degree or diploma in any university; and that to the best of my knowledge and belief it does not contain any material previously published or written by another person except where due reference is made in the text.'

Signed:

Date: 02/02/2017

ACKNOWLEDGMENTS

Firstly, I would like to thank the Almighty God! Jesus thank you so much for life, for your grace and strength that has carried me through to the very end I could not have done it without you! You who started a great work in me has brought it to completion. You are a faithful God, always there for me at every step of the way! Thank you is all I can say. "For God did not give you the spirit of fear but of power, love and a sound mind; and those who know your name put their trust in you, for you Oh Lord never forsake those who seek you" 2 Timothy 1:7 & Psalms 9:10. Secondly, I would like to thank Mr Saulo you have truly been an amazing supervisor to me. Thank you for giving me the opportunity to work on this project that had challenged me both academically and personally which has led to growth. Thank you for your guidance, patience, being understanding, encouraging, always reassuring me, for your wisdom, advice, knowledge, always being available for me, I do not think I would have gotten as far as I did without your hand of support. I am so grateful for your life may the Lord Jesus bless you beyond measure. Thirdly, I would like to thank my family; Mum, Dad, bestie Ruth, Rebecca, Kelliena, Deborah, Nathan, Mary for your incredible love, prayers and support, you have all been amazing in various ways. I love you all and may the Lord bless you all! Fourthly, I would like to thank my prayer team; bro Winsly, Sis Tina and Sis Shekinah, thank you so much for your prayers and being a listening ear! Fifthly, I would like to thank Blesson you have been great, thanks for your prayers, being there, checking my thesis, for taking me along with you to the workshops which were good but never really got to put into practice much what I learnt. Sixthly, I would like to thank all my friends, the old ones as well as the new ones, I did not think I would make friends coming back this year but every one of you have made my journey special. Just a shout out to Deepali, oh it's been a long journey and friendship in the making! I am so glad you have been a part of it. All in all, you have all made my journey one to remember. May God almighty bless you all.

ABSTRACT

For more than a few decades, the investigation of femoral strain has been an active area of study in the biomechanical field. This is because a large number of people are globally affected yearly by femur fracture which is a mechanically related pathology. Therefore, it is vital to understand how strain in the bone is a function of geometry and loads which is dependent on the type of activity the person is performing. This project was privileged to use readily available data from a previous study. The data comprised of twenty-two healthy post-menopausal women aged between 60-77 years who had computer tomograph scans of finite element models taken. Additionally, gait data of weight-bearing tasks such as standing up and siting on a chair, walking up and down the stairs, jumping, walking and fasting walking performed by each subject were also collected.

The aim of this project was to analyse the data available to understand the relationship between femoral strains and activities as this was rather unclear. Two steps were involved; firstly, multiple regression was undertaken to understand the relationship between strain distribution during various activities. Secondly, principal component analysis describing the variations that were possible within geometry was performed. The findings from the multiple regression suggested that daily activities explain 91% of the variations of strains across subjects. Thus proposing that geometry and material bone properties attribute about 9% to the strain distribution in the femur. On the other hand, the findings from principle component analysis indicate that the first 5 modes captured about 93% of the variations of geometry in the training set; this is to state that these modes account for most of the variance in the observed variable. The results obtained in this project demonstrate that the activity a person undertakes is of major importance on the strains exhibited in the femur. However, the results obtained require further analysis to be validated. Nonetheless the next steps in the project would be to incorporate multiple regression analysis and principal component analysis of geometry and material properties to determine the relationship between activities and bone stiffness in relation to strain and determine how simplified information has an impact on strain.

ABBREVIATIONS

CT: Computer Tomography

FEM: Finite Element Method

MLR: Multiple Linear Regression

MSM: Musculoskeletal Modelling

PCA: Principal Component Analysis

SSM: Statistical Shape Modelling

STL: Stereolithography

Tables of Contents

LIST OF FIGURES

LIST OF TABLES

INTRODUCTION

In Australia there are about 4.74 million Australians over the age of 50 years that have been diagnosed with age-related osteoporosis. As a consequence, hip fractures occur because the femur is subjected to stresses beyond its ultimate strength [1]. Age-related osteoporosis is a condition where the process of bone resorption is more rapid than bone formation thereby altering distribution and the amount of bone tissue in the hip; therefore, leading to a decrease in bone density and a bone fragility increase. In the elderly population, osteoporosis is a prevalent disease that increases the risk of fracture fragility and morbidity. Women over the age of 50 years and over are the most affected group as they experience a drop in sex hormone levels with the onset of menopause leading to rapid loss of bone mass and deterioration of skeletal architecture. Thus to understand what is the cause of this age related bone change that leads to fractures, which is a mechanically related pathology the investigation of femoral strain is of importance to be carried out. Therefore, the aim of this study was to investigated how movement during daily activities and femoral strain are related as this is not fully understood. In turn the findings of this project would assist in developing treatment integrated exercises to help reduce femur fractures in the elderly population [2-16]. Femoral strain in the bone is a function of geometry, material properties and loads which are dependent on the type of activities an individual is performing and the manner in which the muscles induce the force on the individual's bone [17].

The study of femoral strain has been performed using in-vitro, in-vivo and in-silico methods with either methods having advantages and disadvantages [18-27]. A study by Tyrer et al. (1995) investigated the strains that are induced in the bone under loads as this would enable the improvement of prostheses and implementation techniques used to design artificial components and the method of the study was in-vitro [28]. Another study by Anderson and Madigan (2013) explored the strain loads in the proximal femur during walking of the elderly, as this has an impact on bone mineral density which is vital in preventing fractures that occur in older people and the method utilised in this study was an in-vivo technique [29]. A study by Jonkers et al. (2004) analysed how the distribution of femoral strain in the proximal femur is impacted by subject-specific geometry and the study was carried out in-vivo [30].

A study by Bessho et al. (2007) examined how femoral strain distribution is related to the loads applied on the femur. As this is essential in quantifying the strength of the femur in order to approximate fracture risk and have preventive interventions. The focus of their study was the strain's proportional function loads and the utilised methods were in-vivo and in-vitro [31]. Another study by Schileo et al. (2007) explored how understanding femoral strain can aid in prediction of fracture risk that occur as a result of the loading conditions applied on the femur. The focus of

their study was the strain's proportional function loads and the method of the study was in-vitro [32]. A study by Duda et al. (1997) investigated how internal forces and moments are exhibited in femur whilst walking. The focus of their study was strain's proportional function geometry and material properties of the femur and the method of investigation was in-vivo [33]. Another study by Edwards et al. (2016) investigated how muscle forces from static optimization and dynamic optimization can be used to predict femoral strain during walking as this would help to decrease femur fractures and improve bone health. The focus of their study was strain's proportional function geometry and loads during an activity like walking. The method for investigation was in-vivo [17].

An investigation by Heller et al. (1998) explored strain distribution caused by muscle forces in the femur. The focus of the study was strain loads induced by the muscle. As this is essential in designing implants and bone modelling for bone resorption which would alter clinical outcomes and the investigation was carried out in-vivo [34]. A study carried out by Koivumaki (2010) examined how strain distribution in the femur coincides with fractures displayed in the femur. The focus of their study was strain's proportional function geometry and loads during a sideway fall. The investigation was carried out in-vivo [35]. Another study by Schulte et al. (2012) focused on the strain's proportional function geometry in terms of how it attributes to femoral strains distribution and the method of study was in-silico [36]. The studies above have highlighted the methods undertaken in the exploration of femoral strain distribution with either method have advantages and disadvantages. Numerous studies have demonstrated that the advantages of using an in-vitro method is that it identifies failure scenarios and can improve a numerical model. The disadvantages of using an in-vitro technique is that it is inefficient in measuring femoral strains on the bone surface, it can only be used with a small sample size using representative loading scenarios, it is time consuming and expensive, affected by experimental, systematic and random errors [37-40]. Whereas the advantage of using the in-vivo method is that patient specific finite element models can be derived. The major disadvantages of the in-vivo method is that strains in the bone cannot be measure without the use of an invasive, only known or suspected scenarios can be investigated, idealisation is implemented to assume true an entity known as being false, every solution is approximated and it is difficult to determine whether or not the models developed are good thus in-vitro method is used as a comparison; in-silico method is the study of models to predict what may occur [17, 41].

As noted above there are limitations with the different study techniques hence making it difficult to understand what is happening inside the bone during various forms of activities. Yet, the study by Martelli et al. (2014) demonstrates it is rather possible to combine all three methods to analyse femoral strains during daily activities. The study investigated the association between femoral strains during a daily activity such as walking. Their findings were that the strains exhibited in a daily activity like walking had an impact on femoral fractures; 46-60% of the strain variance in the

lateral femur could explain whole body dynamics. Thus this study focused on the strain's proportional function loads exhibited in the femur during daily activities. Nevertheless, the study was limited to one subject, a single activity and a single location which was only the points on the lateral side and frontal plane therefore this cannot be extrapolated to the overall population. Hence the undertaken project aimed to investigate strains with regards to various activities, across subjects considering all points [42].

Table 1: This table aims to highlight the focus of previous studies and the methods used

Study	Focus	Study method
Martelli et al. (2016)	Loads exhibited in the femur during daily activities	In-silico
Edwards et al. (2016)	Bone geometry and loads during an activity like walking	In-vivo
Anderson and Madigan (2013)	Bone geometry and loads.	In-vivo
Schulte et al. (2012)	Bone geometry	In-silico
Koivumaki et al. (2010)	Bone geometry and loads during a sideway fall	In-vivo
Bessho et al (2007)	Loads exhibited in the bone	In-vivo and in-vitro
Schileo et al. (2007)	Loads exhibited in the bone	In-vitro
Jonkers et al. (2004)	Bone geometry and loads	In-vivo
Heller et al. (1998)	Loads in the bone induced by muscles	In-vivo
Duda et al. (1997)	Bone geometry and material properties of the femur.	In-vivo
Tyrer et al (1995)	Loads exhibited in bone	In-vitro

Thus all the studies above have explained the importance of understanding femoral strain with regards to tackling fractures that occur in the femur, and from these studies it can be understood that the focus parameters of femoral strain were examined using either geometry, material property or load but what these studies have not explored is how these parameters together relate to strains created in the femur that causes skeletal diseases. Therefore, there is an incomplete established representation of how strains formed in the femur depends on geometry, material properties and loads. In order to establish the relationship between geometry and loads in generating femoral strain, multiple linear regression was firstly used to draw the link between

strains in the femur during daily activities such as jumping, normal walking, fast walking, lifting a chair and walking up and down the stairs. Secondly statistical shape modelling was used to describe the variations in geometry and material bone properties [2-4, 43-45].

Thesis outline;

Chapter 1 provides background knowledge that was essential in tackling the investigation of what is the relationship between femoral strain and movement. It covers the anatomy of the hip joint, anatomy of the femur, mechanical and structural properties of the bone which are all vital in the full operation of the femur and it ends with a description of the techniques used in the previous study to collect the data including the use of finite element modelling and musculoskeletal modelling. Chapter 2 leads to describing the data that was used in making the project possible. Furthermore, the chapter goes on to describe the methodology undertaken in acquiring the results to achieve the objective of the project which was to determine how strains in the femur are attributed to geometry and loads. Chapter 3 discusses the results obtained when multiple regression was performed on every subject's 6 activities and the results observed when PCA was applied to geometry of the femur; lastly the chapter ends by discussing the limitations, future works and concludes the project investigated.

CHAPTER 1- BACKGROUND

This chapter firstly provides a general overview of the anatomy of the hip joint and femur in terms of their structure and the movements that are executed as a result of the anatomical structure of the femur and muscles that are involved.

1.1   Anatomy of the Hip joint

The hip joint is comprising of the femur and acetabulum. It is a congruent ball and socket joint as shown below in Figure 1 that has a joint cavity, cartilage covered surface, a synovial membrane and a ligamentous capsule. The hip joint is surrounded by powerful and well-balanced muscles as shown in Table 2 and Figure 3 that are providing a wide range of motion in several physical planes. In particular the sagittal plane is where the range of motion is greatest as shown below in Figure 4. The hip does all of this whilst maintaining remarkable stability because of its anatomic congruity. It also transmits forces from the ground up as well as carries forces from the trunk, head, neck and upper extremities [46]. The hip joint possesses mobility within six degrees of freedom, which are flexion, extension, lateral rotation, medial rotation, abduction and adduction. [47, 48].
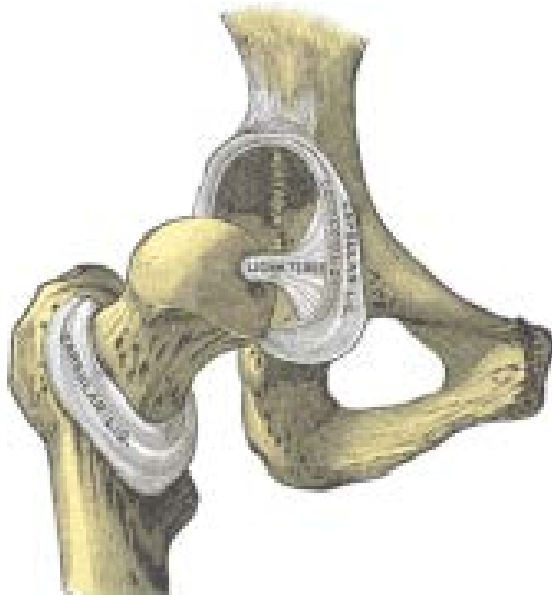
Figure 1: The hip joint [49]

Table 2: Muscles in the human body [50]

Hip position	Primary muscles	Secondary muscles
Flexion	Iliopsoas Rectus femoris Tensor fascia latae Sartorius	Pectineus Adductor longus Adductor magnus Gracilis
Extension	Gluteus maximus Biceps femoris Semitendinosus Semimembranosus	Gluteus medius Adductor magus Piriformis
Adduction	Pectineus Adductor brevis Adductor longus Adductor Magnus Gracilis	
Abduction	Gluteus medius Gluteus minimus	Gluteus Maximus Sartorius Tensor fascia
Lateral rotation	Obturator internus and externus Gemelli superior and inferior Quadratus femoris Piniformis	Gluteus medius Gluteus minimus Gluteus maximus
Medial rotation		Gluteus medius Tensor fascia latae

Figure 2: Joint motions [51]
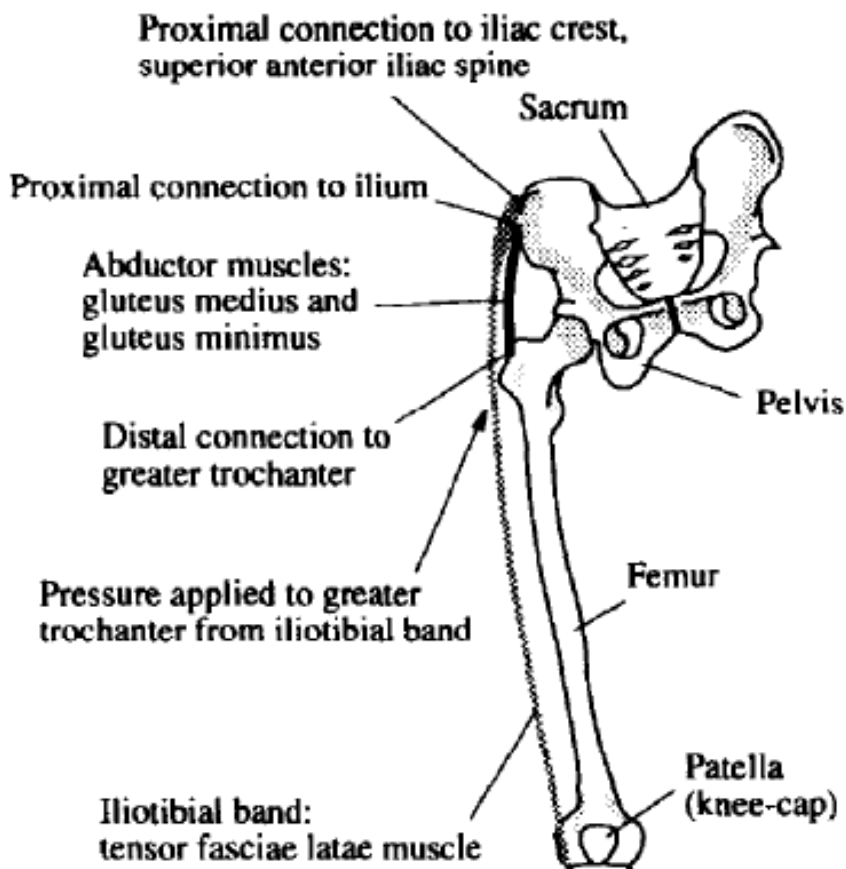
Figure 3: Major muscles that act on the femur [29]
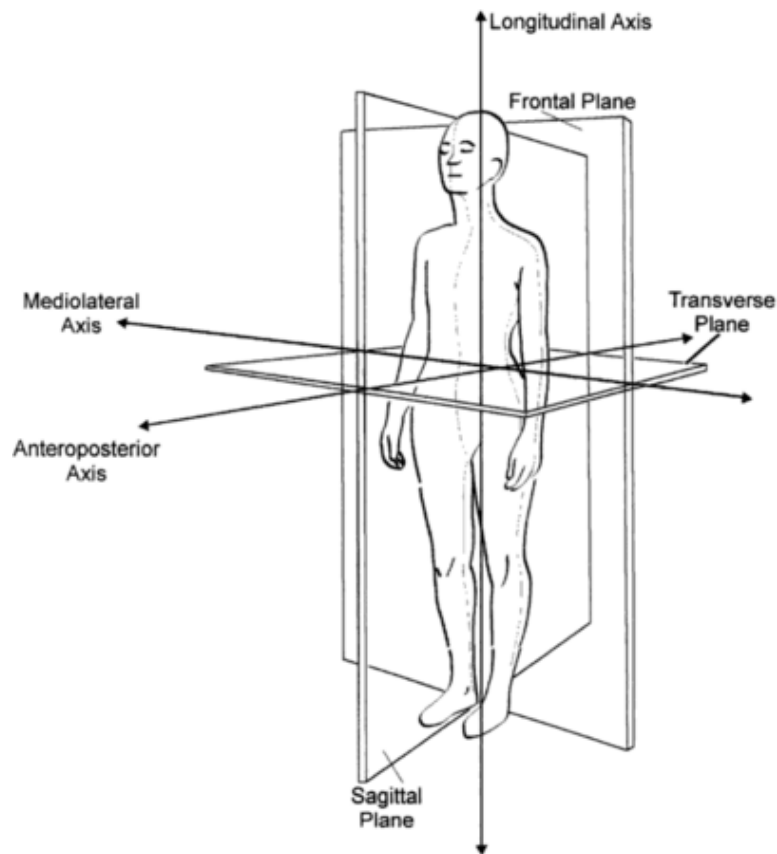
Figure 4: Anatomical planes of motion and axes of rotation [52]

1.2 Anatomy of the femur

One fundamental bone in the human body is the femur. The femur is the longest bone and the strongest bone in the skeletal system. The femur is divided into a shaft and two extremities. The upper extremity comprises of the femur head, neck and greater and lesser trochanter as shown in Figure 5. The shaft which is the corpus femoris and the lower extremity comprises of condyles. The femur taken together forms a single mechanical structure well-adapted for efficient and economical transmission of loads from the acetabulum to the tibia for maximum mechanical efficiency [53]. The proximal tip of the femur comprises of both the compact bone and the sponge bone. The compact bone covers the external part of the bone and goes downside forming the bone body. Whereas the sponge bone is found in the tips and the principal orientation of the trabeculae bone are aligned with the main loaded direction. The femur exhibits anisotropic characteristics therefore according to the forces applied to it in different directions it will respond different [54].

Hence in the longitudinal direction of the femur greater forces are applied, its stronger when forces are applied longitudinal and it weaker when the forces are applied transversal crossing its surface. Compressive strengths are experienced at the femur which is essential for its development and

growth. However, it is good to note that a compressive strength of approximately 3-7 times the body weight during walking is absorbed by the hip joint. In a normal body standing posture, the hip joint takes about three body weight. With all of its structure, the femur participates in supporting the weight in the lower limbs and is strongest when the load is coming from a compressive strength as previously mentioned. The femur displays higher tensile strength capacity of the middle slope of the body [54-59].
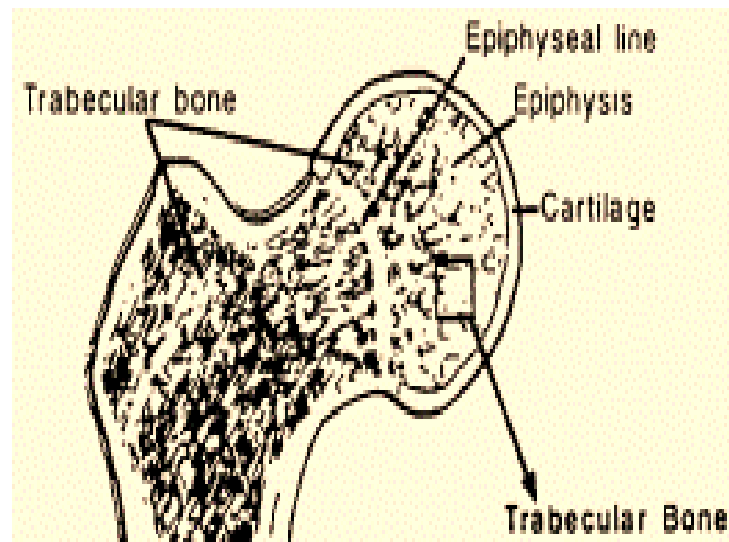
Figure 5: Trabeculae bone [35, 60, 61]

1.3   Mechanical properties of the femur

Bone is a dynamic structure that exhibits adaptation to changes in its biochemical and biomechanical environment [14]. It is a specialized form of connective tissue, in the human body its functions are to provide mineral ion homeostasis, structural support, protection and storage of healing cells; hence it has a varied arrangement of material structures [62]. The cellular makeup of bone are osteoblasts, osteocytes, bone lining cells, osteoclasts and inorganic and organ component [8]. The microstructure of bone in the femur comprises of the cortical bone and the cancellous bone. The cortical bone is a cylindrical shaped lamella, is less porous but highly dense compared to the cancellous bone. Therefore, the cortical bone forms the outer layer of the femur whereas the cancellous bone forms the interior part of the femur [62]. The cancellous bone is made up of trabecular struts and cavities that are filled with bone marrow. The mechanical properties of the cortical bone are subject to the orientation and direction of osteons. Whereas the mechanical properties of the cancellous bone are subject to density and location. The cortical bone has higher strength in compression than in tension and the elastic property of the cortical bone depends on type of loading and direction [62].

**Table 3: Mechanical properties of the cortical and cancellous bone [63]**

Property	Cortical bone	Cancellous bone
Compressive strength (MPa)	100-210	2-12
Tensile strength (MPa)	50-150	10-20
Strain to failure (%)	1-3	5-7
Fracture toughness (MPam$^{1/2}$)	2-12	-
Young's modules (GPa)	7-30	0.5-0.05

1.4 Finite element modelling of the femur

Computer tomography (CT) is used to reconstruct a cross-sectional image of the internal human body. In other words, it is a cross-sectional image representing in each pixel the local X-ray attenuation properties of the body. CT is used in biomechanics as a method to retrieve the geometry of bones and local material properties. Calibration phantom are used to link the pixel attenuation values of the scans to a standardized unit of measure. Therefore, from the grey scale values of different phantom materials in the images a relationship between mineral content and CT attenuation values can be obtained. The calibration coefficients can be derived from the phantom. The pixel value of the image provides a measure of how much radiation has been attenuated in the material at the site of the pixel, which is the linear attenuation coefficient. The pixel values are specified in Hounsfield units, thus they are normalised with regards to the linear attenuation coefficient in water.

CT imaging as shown in Figure 6 works by a thin collimated beam of X-rays that pass through the body to a detector that measures the transmitted intensity. The collimator is a set of narrow lead tubes which results in a straight beam of X-rays. As the source and detector are moved past the body together measurements are made at a large number. For the image to be formed from a CT the width of each pixel is chosen in accordance with the width of the detectors or the width of the X-ray beams. This determines the resolution of the image; the X-ray detector only measures the intensity of the transmitted beam after it has passed through the body, the value gets subtracted from the intensity of the beam at the source to produce the total absorption; which is the only absorption that is measurable along each beam line. From this a grey value is assigned from each pixel according to the amount of radiation absorbed. The x-rays are produced when the electrons

are accelerated in an electric field which is determined by an electric potential. All in all, the reason that CT image datasets are utilised when it comes to the application of musculoskeletal modelling and finite element modelling is because CT image datasets are accurate and informative. Particularly when it comes to understanding how strain distribution in the femur is contributed by geometry and loads. This is irrespective of the fact that CT scans are quite costly and the subject would have a high dose exposer of ionizing radiation. The dosage given to the subject is dependent on the geometric efficiency, which is the fraction of transmitted x-rays that interact with the active detector area. As well as the absorption efficiency which is the fraction of x-rays interacting with active detector areas that are being captured. [64-66].
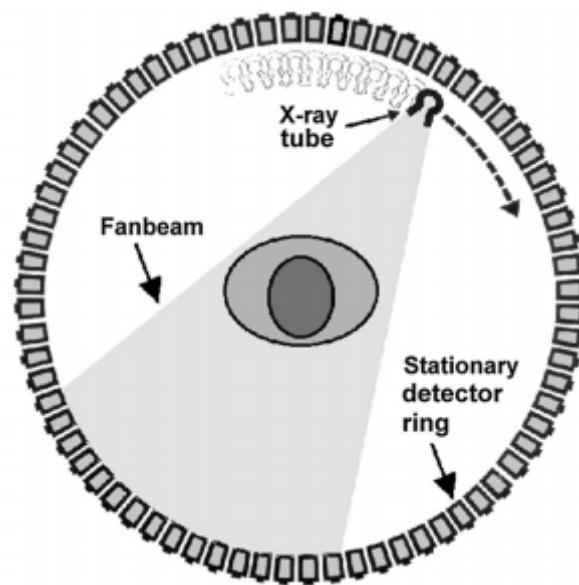
Figure 6: 4th generation CT scan [65]

Finite element modelling (FEM) is a simulation technique that involves the breaking of continuum into discrete, coupled components to estimate the overall solution of the problem. It was first introduced in bone biomechanics in 1972. Since then for the past decades' FEM has been used in bone biomechanics to analyse strain in the bone, as it is a non-invasive technique and can be used to model subject specific geometry of the bone using computer tomography (CT) data [30, 67-69]. The major steps involved in this process are pre-processor, solution and post process.

The pre-processing stage is where the element types to be used are considered which may comprise of degrees of freedom, number of nodes, formulation and integration and axisymmetric elements that provide the modelling bodies of revolution under axial symmetric load conditions. For an FEM model of the femur to be created, the bone needs to be segmented from a CT scan image, then meshed into comprehensible format for the FEM model. CT imaging is used in FEM because subject specific models can be generated. The process involves firstly calibrating the CT data using Hounsfield units to the apparent femur bone. Next the density of the bone [70].

Segmentation as shown in Figure 7 is when images from CT are divided in parts similar to their characteristics. The segmentation is performed either manually or semi-automatically using grey scale values linked to material distribution and outer contour definition to isolated bone from its surrounds. This then leads the femur to be exported to an FEM software representing the original femur bone in the form of an element mesh. The mesh is either tetrahedral or hexahedral. Material properties are implemented to the segmented bone using the data derived from a CT image. Each element contains a grey value of its own enabling the implementation of heterogeneous material properties to the mesh [71]. The geometry of the femur bone can be generated using computer tomography. In order to produce accurate FEM results it is vital that exact boundary parameters are applied as shown in Figure 8 [72, 73]. This is for the purpose of the femur bone to simulate realistic physiological activities; thus boundary conditions are implemented before analysis can begin. The conditions of the properties are those that are superficially situated to a system which can be applied to the nodes and elements of the FEM model to simulate the behaviour of the system in space. Then after this strain distribution can be calculated [74].
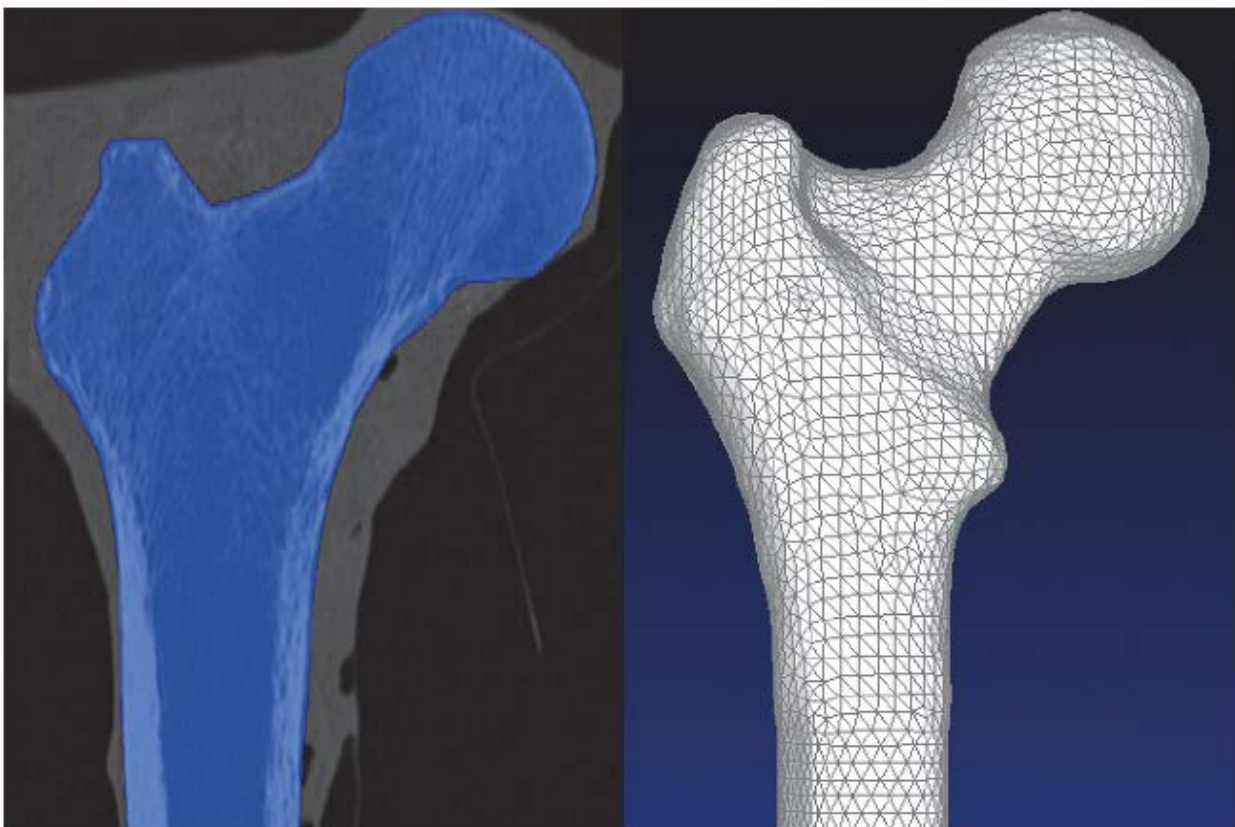
Figure 7: Segmentation of the femur bone from a CT scan

In summary the steps involved in FEM are [75];

1. Discretise the continuum
2. Interpolation functions selection

3. Find element properties
4. Assemble element equations
5. Solve global equation system
6. Compute additional results

As previously mentioned to create an FEM model, the model has to be segmented from a CT scan and the material properties are based on the CT image. The model is then mesh refined and subject specific models of the femur are created by adjusting the geometry and material properties of the femur model based on subject femoral geometry [29]. Figure 8 displays the phases involved in developing a finite element model.
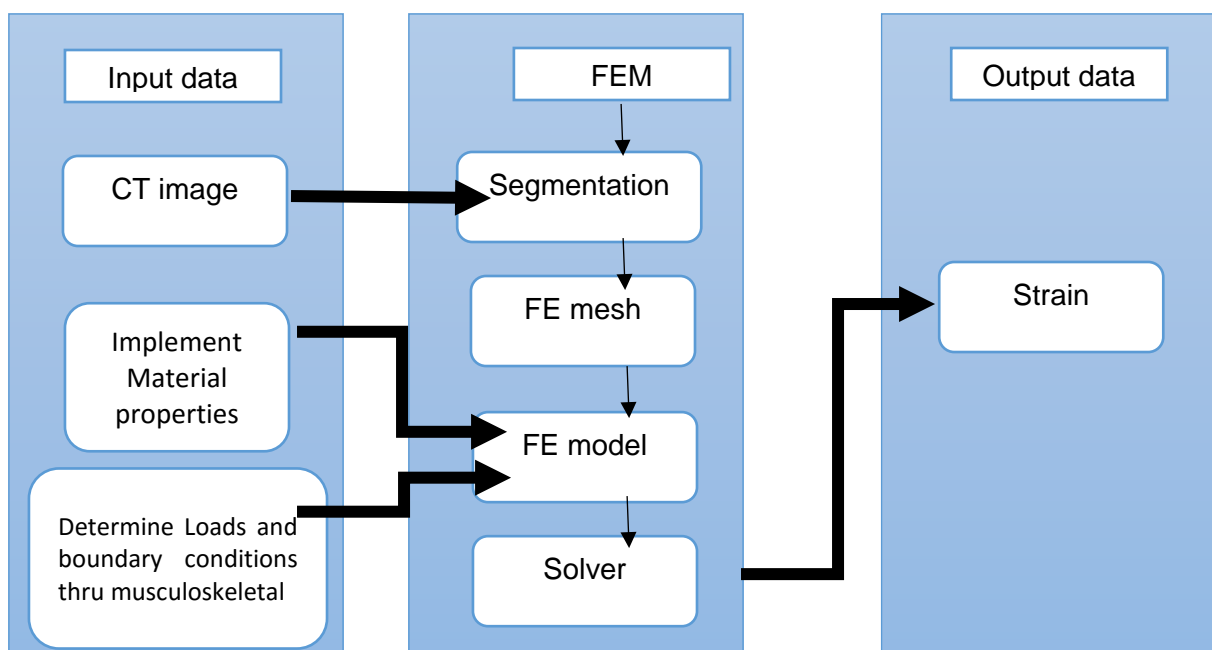
Figure 8: FEM of femur bone based on CT imaging [74]

1.5   Muscle and joint forces during activity

Musculoskeletal modelling technique has been used in various studies to model the estimate internal loadings on the human body which is not possible to measure directly in vivo from external measurements such as kinematics and external forces [17, 30, 42, 76-79]. Hence it is able to simulate the movement dynamics that is produced as the elements of the musculoskeletal system interact through gait analysis. This technique assumes the musculoskeletal system to be a mechanism of rigid segments connected by joints and actuated by Hill-type muscles. The method enables the creation of a detailed human body calculation model that incorporates all the vital components of the musculoskeletal system. Two methods are combined with musculoskeletal methods these are inverse dynamics and forward dynamics. For the purpose of this project

inverse dynamics was used to simulate the human body as a mechanical system. Inverse dynamics was implemented as motions and external loads on the human body were known, thus the purpose was to determine inertial forces such as joint moments and joint reaction forces. The advantage of using inverse dynamics is simply that the computational efficiency allows for realistic models of the body that comprises of more than 300 muscles as shown in Figure 9 [78]. To generate a musculoskeletal model, a three dimensional bone surface geometry, mathematical descriptions of joint kinematics, parameters describing each muscle's path geometry and muscle architecture are collected as inputs from a cadaver. Then from these factors the model can be created and used to estimate muscle lengths, moment arms, muscle forces and joint moments for any arbitrary set of joint positons. At that point the models are evaluated by comparing muscle moments arms with a cadaver's measurements of moment arms and maximum joint moments with experimentally measure joint moments. Figure 10 displays the musculoskeletal modelling procedure [80].

Figure 9: Model of the human body comprising of more than 300 muscles [78]
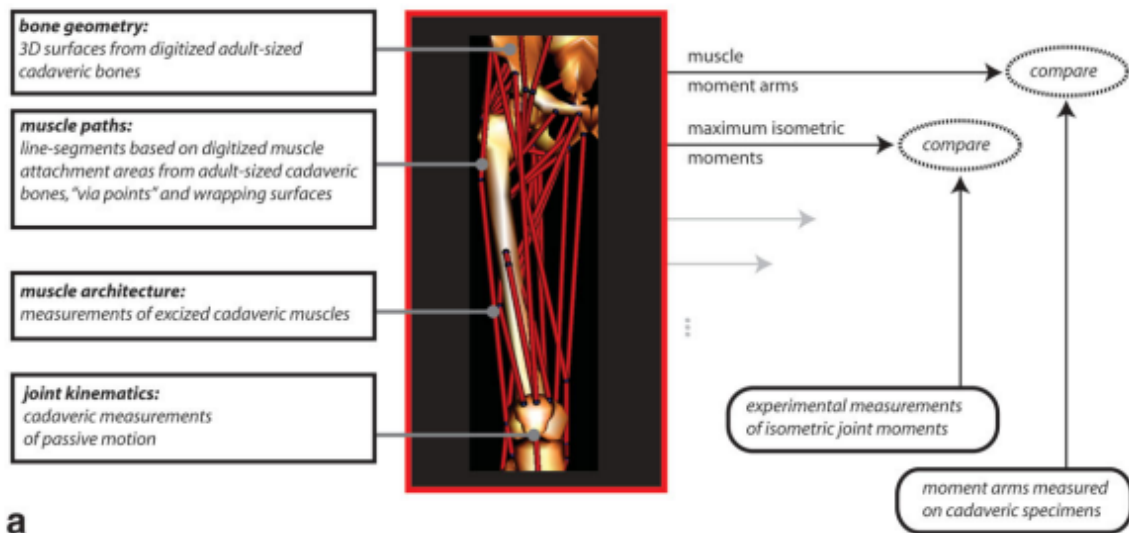
Figure 10: Phases in the musculoskeletal modelling

Gait Analysis is the systematic study of human locomotion. Through gait analysis kinematic and kinetic data are acquired. This provides a fundamental understanding of what goes on when a person walks in particular when they are performing weight-bearing activities such as jumping, lifting a chair or walking up the stairs as shown in Figure 11 [81].
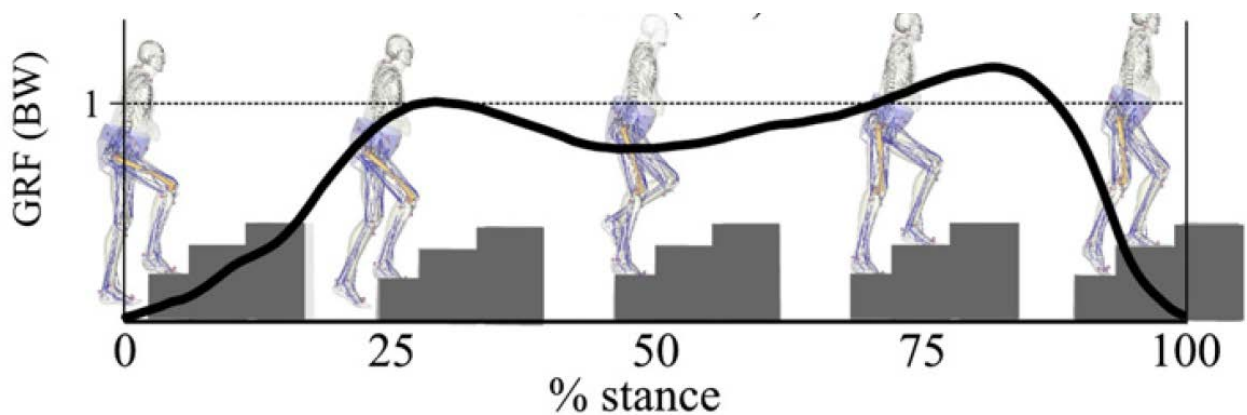
Figure 11: Gait analysis during stance phase of walking up the stairs [42]

All the techniques mentioned above are inter-used for the sole purpose of developing models of the bone in vivo to be able to predict how strain in the femur is related to factors such as geometry, material properties and loads.

CHAPTER 2- METHODOLOGY

This section outlines the data used and the methods undertaken in acquiring the results to achieve the aim of the present study was to investigate how strain distribution in the femur is dependent on geometry and loads which are dependent on the activity the subject is performing.

2.1   Femoral strains during activity in elderly Caucasian women

The data utilised in this study was taken from a previous study that comprised of twenty-two healthy post-menopausal women aged between 60-77 years of age who walked unassisted and had no history of musculoskeletal disease [77]. The data encompassed twenty-two STL files (Figure 12) that contain femur models which were used to acquire the PCA geometry of femur. There were twenty-two inverse dynamic files for various activities such as standing up and sitting on a chair, fast-walk, jumping, stairs up and down and normal walking that were in an STO format. An STO format is simply a file format that the inverse dynamic files were stored in. The STO files contained the various moments at the hip such as flexion, extension, rotation and moment at the knee and ankle. There were also files that contained processed results of all the subjects in a Matlab variable that had the strains of the various activities. As such this was a great opportunity to attempt to understand how the anatomy, the way humans walk, what activities they are engaged in are all interconnected. As this knowledge would open new avenues which would strategically tackle pathologies such as osteoporosis which is growing into an economic and social burden for the society. **Please do note that the same subjects were used for PCA and multiple regression analysis.** The techniques that were employed in the course of the study to understanding the relationship between femur mechanics and movement is outlined below.
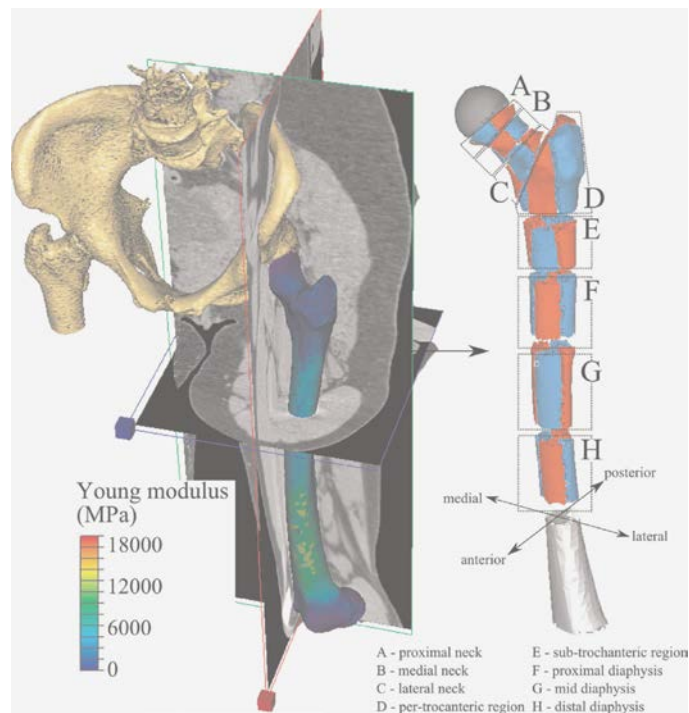
Figure 12: FE model of the femur created from CT images. It shows the different regions of the femur [77]

2.2 Methodology

2.2.1 Data collection

CT scans of each pelvic and thigh areas were collected with a clinical full body scanner and an axial protocol scanner. Two datasets of monochromatic image were attained of the scan. The datasets of the femur were then reconstructed using an in-plane transverse resolution, whereas the reconstruction of the pelvis dataset was performed with an adjusted in-plane transverse resolution to ensure the entire pelvis was accommodated. A five sample phantom calibration was positioned beneath the dominant leg while scanning [77]. The gait analysis experiments were conducted at the university of Melbourne. Forty-six skin-mounted reflective markers were placed to the anatomical locations such as the pelvis, thigh, shank and foot with the rest of the markers being attached alongside the upper extremities and torso. The marker trajectories were filmed with a motion capturing 10 camera system sampling at 120 Hz. Each of the subjects were directed to perform weight bearing activities at a self-selected speed. For instance, they had to walk at a self-selected pace, walk at a faster self-selected pace, go up and down a flight of 3 steps at a total height of 16.5 cm at self-selected pace whilst ascending the first step of the stairway using their dominant foot; stand up and sit on a chair height of 47cm and jump as high as they possible could from a comfortable upright position with each of their foot positioned on a separate force platform. Each task execution was repeated five times. Three strain gauged force plates were used to record ground reaction forces and moments at a sampling frequency of 2000 Hz [77].

2.2.2 Musculoskeletal modelling

In this project the scaled generic musculoskeletal models were used as shown in Figure 13. The models were based on a generic model that was developed by Dorn et al. [82]. The generic model comprised of twelve segments with thirty-one independent degrees of freedom that were actuated by nine-two Hill-type muscle-tendon units as shown in Figure 13. The lumber joint, each shoulder and hip were represented by the ball and socket joint. The knee was represented by the translating hinge. The ankles were represented by a universal joint. Ten ideal torque motors actuated the shoulder and elbow whereas actuation of the other joints was by Hill type muscle tendon units. The scaled generic models used in this project were acquired through scaling of the generic model in order to match each body anthropometry and mass with the help of OpenSim. In order to scale bone geometries, joint centres, joint rotation axes, muscle paths, fibre lengths and tendon slack lengths inter-marker distances were used to record during static trial. By maintaining the mass ratio amid segments in the generic model the mass of the generic model was scaled to match that of every subject. The muscle paths in the scaled generic model were registered on the skeletal surfaces by overlaying the muscle lines of action onto the CT data. The scaled generic muscle was calculated for the dominate leg of a selected trial.
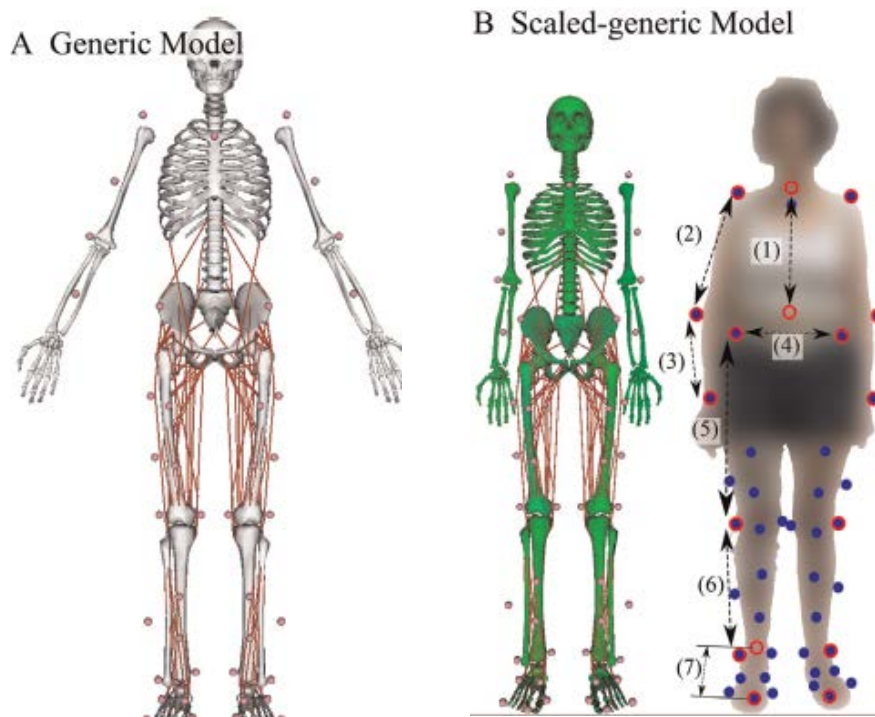
Figure 13: Generic model (left) and scaled generic model (right)

2.2.3 Finite element modelling

Ten node tetrahedral elements were used to model the tissue in the bone. A linear regression equation linking the grey levels in the CT dataset to the hydroxyapatite density in the five sample calibration phantom was used to alter the grey levels images into actual bone density levels. The apparent bone density distribution was altered into an isotropic Young's modulus values for every voxel with implementation of the relationship as derived by Morgan et al. Young's modulus values were incorporated over each mesh element with the use of Bonemat (computer software that maps on FE mesh elastic bone properties obtained from a CT image). The femur was divided into eight different levels. Each level was then further partitioned into four regions such as anterior, posterior, medial and lateral aspects, making a total of 32 subregions as shown in Figure 12. The finite-element model of each femur was kinematically constrained at the femoral epicondyles, which is statically equal to applying forces acting on the most distal femur. To avoid boundary condition artefacts five elements layers surrounding the muscle attachment points were excluded. The scaled generic muscle was applied to the finite element model using custom code developed in Matlab.

2.2.4 Multiple linear regression

To model the correlations between strain and various activities (from standing up and sitting on a chair, jumping, walking up and down the stairs, normal walking and fast walking) multilinear regression (MLR) was used. The purpose of using MLR is to model the relationship between several predictor variables vs criterion variables by fitting a linear equation to the observed data as shown below [83].

$$y = \beta_0 + \beta_1 x_1 + \beta_2 x_2 + \beta_3 x_3 + \ldots + \beta_k x_k + u,$$

β_0 is the intercept, β_1 is the parameter in relation with x_1, β_2 is the parameter in relation with x_2 and so forth. In relation to this project, β was the strain parameter in the bone during various activities in association with x which were the moments as shown in Figure 14. When performing multiple regression other factors that were of interest were the coefficients, R^2 (correlation coefficient), peak error and root mean square error (RMSE) [84].
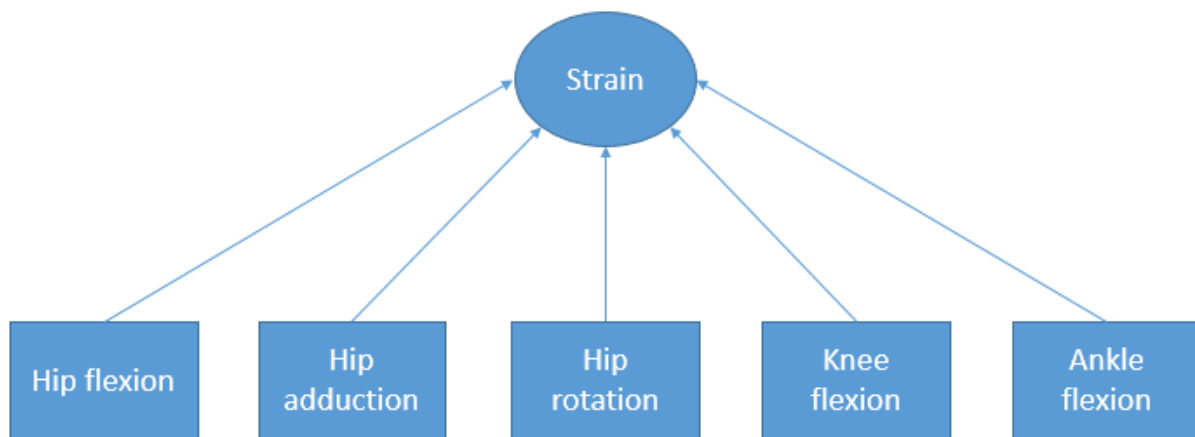
Figure 14: Multiple regression model strain is the dependent variable and the moments are the independent variables

2.2.5 Statistical shape modelling

Statistical Shape Modelling (SSM) aims to capture variations that are possible within a class of shapes through analysis of the training set of data. SSM is used to establish correspondence between a set of shape surfaces on either 2D or 3D; as it is an effective method to parameterise the studied variability and constructing a solid representation of shape. SSM can also be described as a technique that analyses and models on a set of sample shape vectors, the variation of shape across the population using principal component analysis. This technique is widely used in image registration. Image registration is the process by which medical imaging data is aligned in order that comparisons could be made [85, 86].

Studies have shown that anatomical variability and strain properties are important. Therefore, to understand what occurs in a population of interest such as post-menopausal women; and to be able to describe what happens in the overall population, the gap needs to be bridge between single models based on CT scans to the population and one way of doing this is SSM. SSM takes specific points distributed within a population and describes a continuous variation of the population. SSM can be constructed using various methods but Principal Component Analysis (PCA) is the method as demonstrated by Cootes and Taylor. They illustrated that a model using

PCA can be trained on a set of possible shapes and the outputs could be used to investigate the main modes of variation in the set of training data and also to generate new and accurate occurrences of the shape. PCA is a point to point correspondence established through the use of active shape models or active appearance models [87-89]. Active shape models are model-based techniques that aim to match a set of model points to an image that is constrained by a statistical model of the shape. Whereas active appearance models aim to match the position of the model points as well as the depiction of the texture of the object to the image; thus the main idea behind them is to use PCA to derive shape variations from the training set [90]. Additionally, active shape modelling is used in instances such as where given a training set of shapes, each is represented by a set of points, a linear model is derived that describes any new shape as the sum of mean and a weighted combination of modes of variation. The weights are what is called appearance, give a compact encoding of any particular shape with way less modes than points using this approach material properties of the femur may be modelled [91].

PCA enables the building of statistical shape models of bones and joints [92]. It is a statistical method that enables the organisation and reduction of data in order to provide few modes with the highest variations with the training set. The aim of using PCA is to determine and show the relationship amongst several components of uncorrelated variables such as the principal modes of shape variation. It does this by data reduction providing a more specific meaning to the components, therefore enabling interpretation of the data components in a sensible manner. However, it is important to note that the first components produce the highest correlation between the components which is distinguishable and has larger total variance[85, 93]. Figure 15 shows how PCA works, it rotates the axe of the components and changes the value of the components as a result the values of the components are correlated. Therefore, the biggest variability makes interpretation possible [93]. The benefits of using PCA is that it performs data reduction and also the modes obtained from the PCA can be optimised to fit the model to a new individual this is known as active shape model [85].
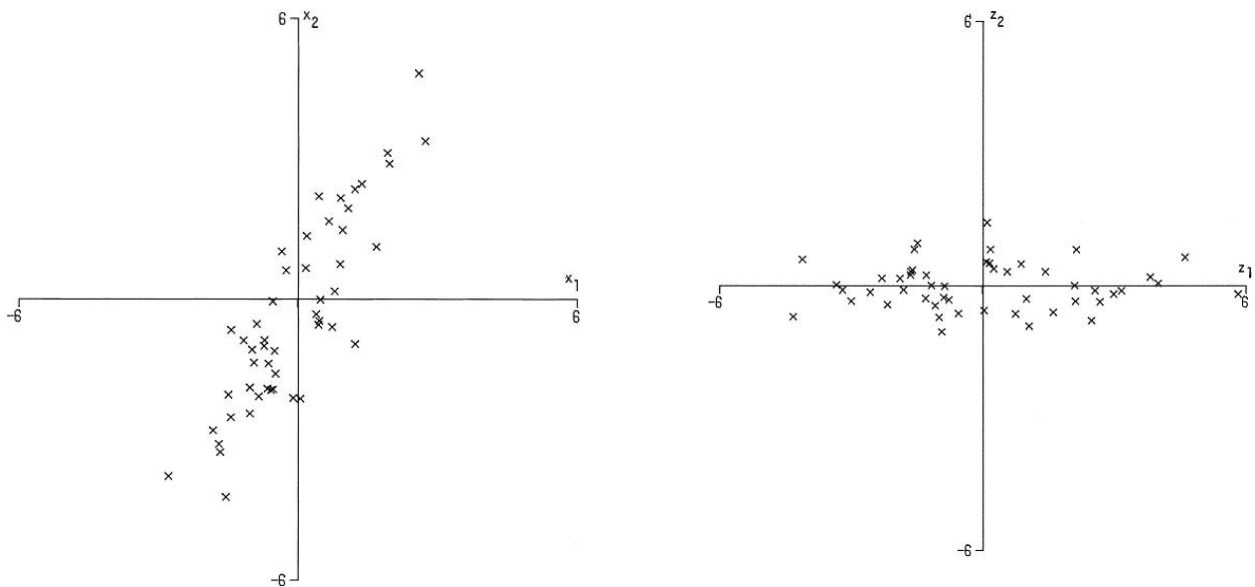
Figure 15: Plot of 50 observations on two variables x_1, x_2 (left), plot of the 50 observations with respect to their components z_1 and z_2 (right) [94]

As shown in Figure 15 the left graph displays that the observations of x_1 and x_2 are vastly correlated variables even though its more in the direction of x_2 than of x_1 whereas when transformed to principal components z_1 and z_2 (right graph) there is a greater variation in the direction of z_1 than in both the original variables and z_2 has very small variation. This is just to demonstrate that when p has more than 2 variables there would be tremendously correlations therefore the first few principal components should account for most of the variations that were in the original variables [94]. Nevertheless, if the first 3 modes of the PCA were extracted for instance the first 3 modes of a femur below is what would be obtained; mode 1 demonstrates scaling effects of the femur, mode 2 demonstrates thickening of the bone and mode 3 demonstrates increase in femoral head diameter [87].
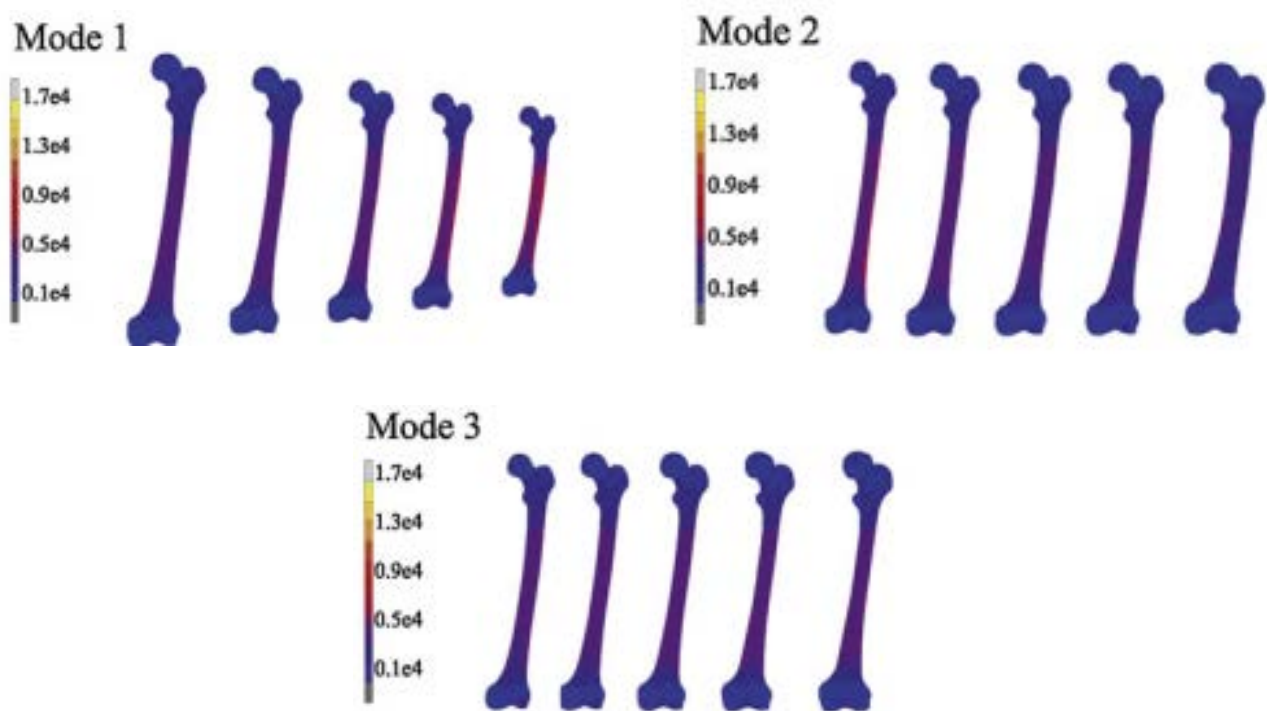
Figure 16: The first 3 modes varied between ± 3 standard deviations [87]

The reason that Multiple regression and PCA were used in the project is due to the fact that in multiple regression multicollinearity occurs when there are near-constant linear functions of more than two of the predictor. Thus, it leads to large correlations between subsets of the variables, therefore the estimated regression coefficients may be large causing instability and distortion of the regression equation. However, one approach to overcome this issue is to use principal components of the predictor variables which in this case is moments in place of the predictor variables as they would be uncorrelated to each other. Thus there would be no multicollinearity consequently simplifying the regression calculations and the regression will be numerically much stable [95]. Additionally, PCA was used because it provided the variations that are possible by using only a few modes whereas Multiple regression represents the loads on the bone of every subject during daily activities.

2.3 Method

Two main steps were carried out in the project. Firstly, multiple regression analysis of the subjects was executed and secondly PCA on the geometry of the femur was performed. Figure 17 is a flowchart that outlines the data files types used to perform the methods previously mentioned. Multiple regression analysis and PCA were all implemented with the use of Matlab. Matlab stands for matrix laboratory and it consists of five main parts which are the Matlab language, working environment, handle graphics, mathematical function library and application program interface. Matlab is an extraordinary performance language used for technical computing, as it assimilates computation, visualization and programming in an easy to use environment using mathematical

notations to express problems and solutions [96].
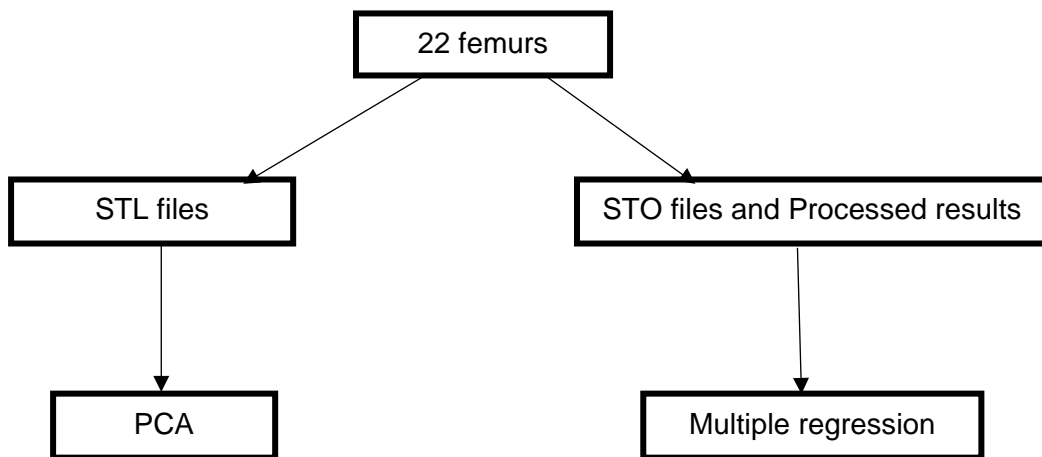
Figure 17: Flowchart of the date files used and methodology undertaken

2.3.1 Determining the relationship between activity and strain

The code that was used to extract the x variables that contained the moments and the y variables that contained strains can be found in the appendix. From the regression coefficients, R^2, RMSE and peak error where derived. Then a graph was plotted as shown in Figure 20. From there a strain map of the activities such as walk and stair-up were plotted to demonstrate the areas of strains that were investigated in this project as shown in Figure 21. This was done for every subject and every daily activity. Below is structural breakdown of the steps undertaken at each stage of the project
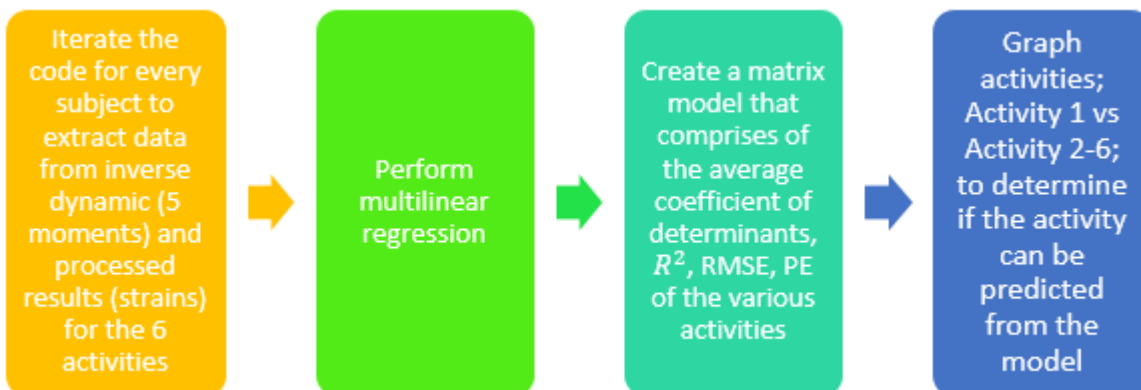
Figure 18: Illustration of the steps undertaken to perform multiple regression

2.3.2 Anatomical physiological variability in the human femur in Caucasian women

In order to obtain statistical modelling of the femur shape firstly dimensional femur models were generated to create a training set. This read the STL files which comprised of the nodes that were

used in getting the dimensions of the femur in order to create the training set. After all the nodes for twenty-two subjects was collected and saved in the format of .txt. A code was run to generate the dimensions of the various locations of the femur used as input for PCA. The output was utilised in creating the PCA matrix input that comprised of femoral length, the distal dimensions, proximal dimension, femoral shaft area, femoral head and neck radius. Then the PCA matrix was used in the Matlab function princi to generate the PCA graph as shown in Figure 22; Overall the STL files were read which led to the generation of femur dimensions that were used as an input to the PCA matrix.
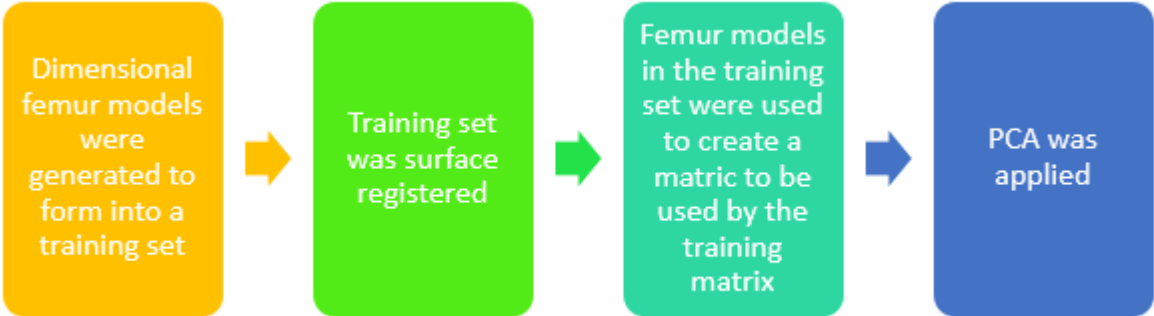
Figure 19: shows a breakdown of the steps undertaken to obtain PCA

CHAPTER 3- RESULTS, DISCUSSION, LIMITATIONS AND CONCLUSION

This chapter provides the results obtained when multiple regression was performed on every subject's 6 activities and what was observed when PCA was applied on the geometry of the femur. It then leads to discuss the limitations, future works and concludes with the aim of the project undertaken.

3.1 Results discussion, limitation, future work and conclusion

The aim of the present study was to investigate how strain distribution in the femur is dependent on geometry and loads which are dependent on the activity the subject is performing. Firstly, multiple linear regression was used to analyse the relationship between femoral strains in the femur in relation to weight bearing activities. Secondly, PCA was used to describe the variations in geometry of the femur.

3.1.1 Relationship of strain across daily activities

Multiple regression was performed to determine what is the relationship between strains (dependent variable) of the bone with the moments hip flexion, hip adduction, hip rotation, knee flexion and ankle flexion (independent variables) during various daily activities such as lifting a chair, normal walk pace, fast walk, jumping and going up and down the stairs of 22 subjects; Please note that the multiple regression results are pilot results. The graph below aimed to draw a relationship between strain distribution in the femur with regards to the activities being engaged in. The multiple regression was created to include for each bone only the loads exhibited during daily activities. From the graph in Figure 20 it was found that activities explained 91% of the variations of strain across subjects as $R^2 = 0.91$. This would mean that geometry and material bone properties attribute about 9% of the distribution of strain in the femur. Figure 21 displays the residual of the strain difference between FEM and MLR, as seen in the graph the residuals have an average equal to zero. The residuals were simply calculated by subtracting the actual values from the predicted values which in this case was strains from the FEM subtracted from strains from MLR. This then led to the calculation of the root mean square error (RMSE). Table 4 shows the calculated RMSE; the RMSE measures the variance of the residuals in regards to how close the actual values are to the model's predicted values. Figure 22 displays the area of interest of strain distribution in the femur. Figure 23 shows the calculated strains from MLR.
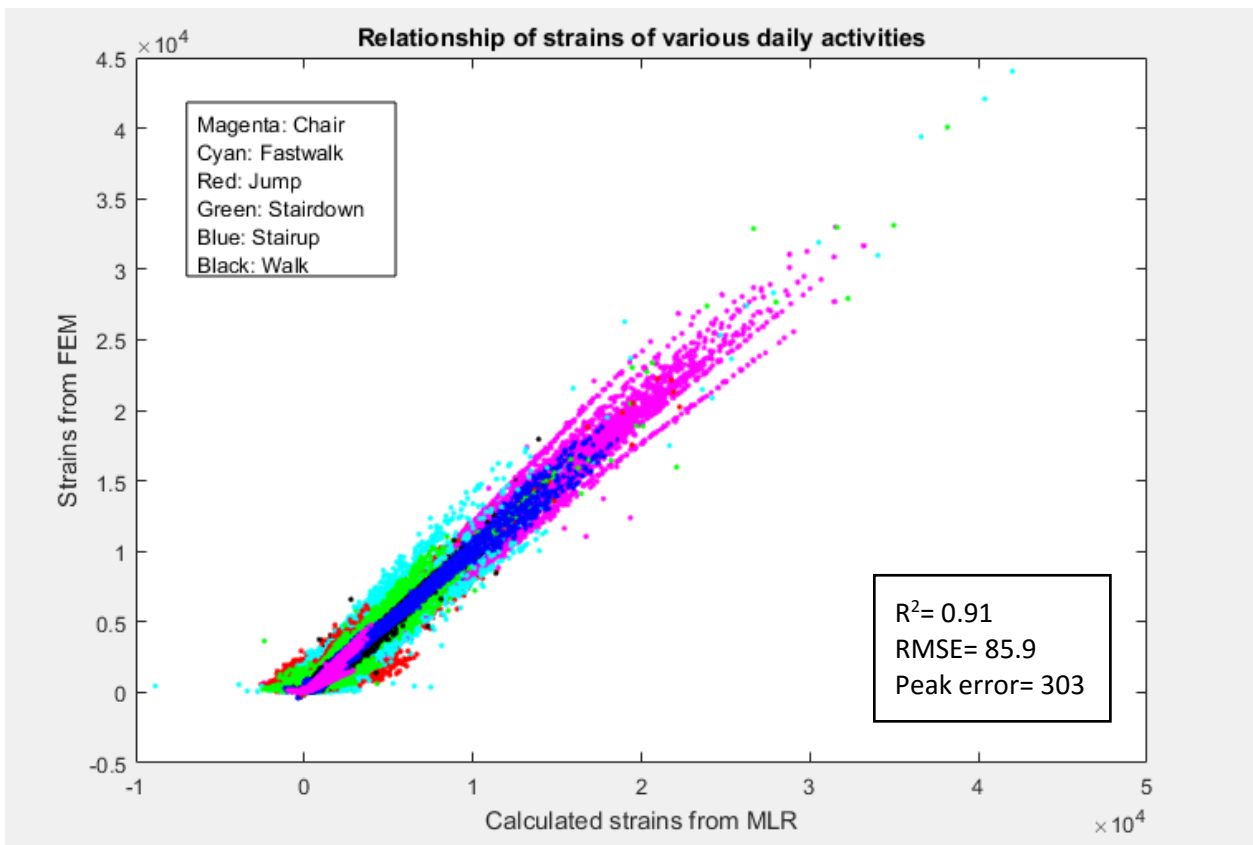
Figure 20: Overall strains of daily activities
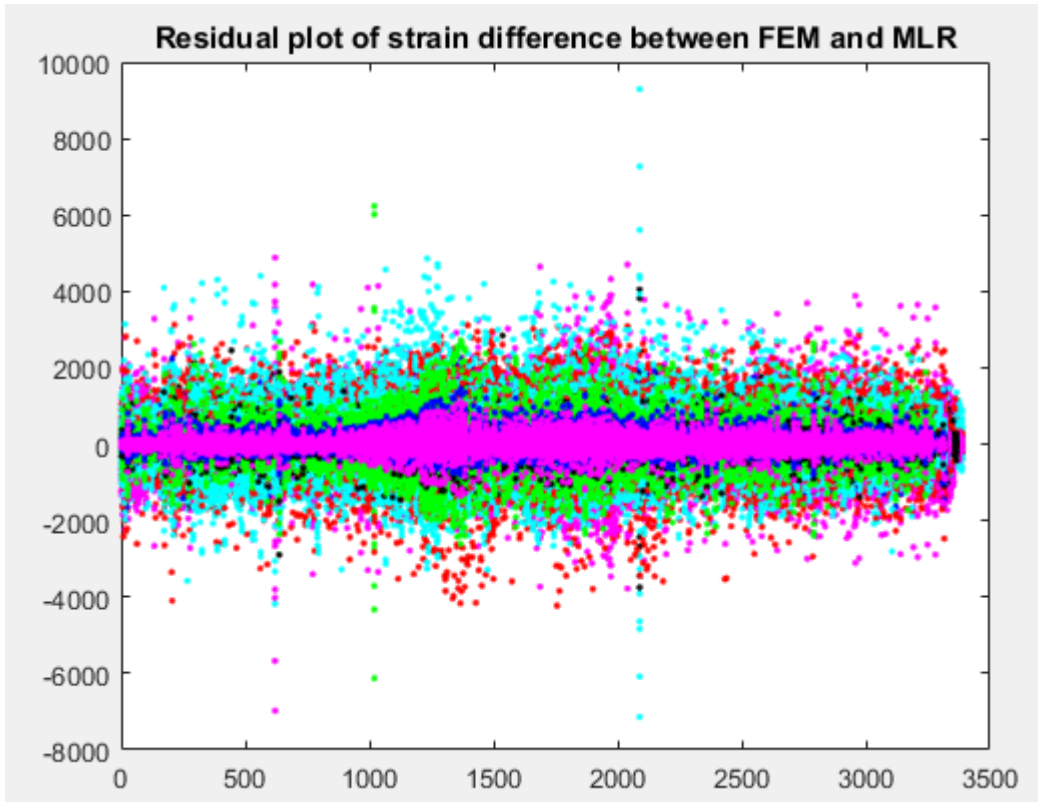
Figure 21: Residual plot

Table 4: RMSE error

RMSE	170.93	71.83	111.53	82.60	103.35	210.81	91.51	132.33	124.22	114.91
	75.61	91.23	95.70	42.25	54.15	62.05	40.09	141.84	117.28	
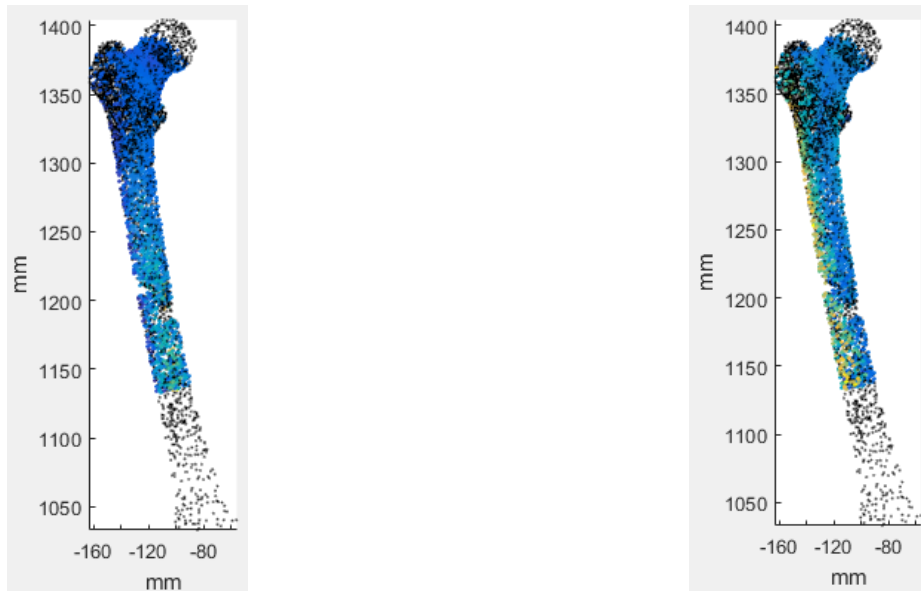
Figure 22: Strain mapping of both normal walking (left) and stairs-up (right)
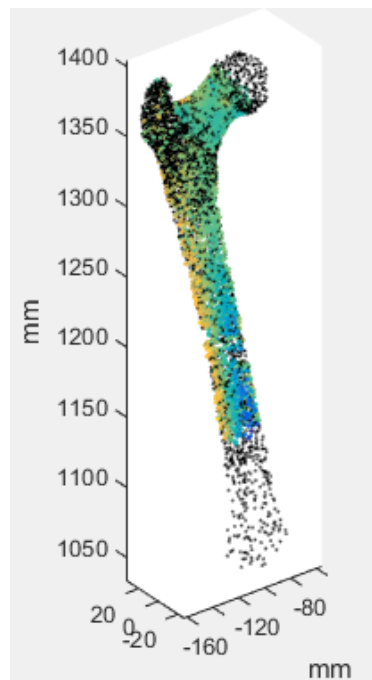
Figure 23: Strains mapping of multiple regression from standing up after sitting on a chair

3.1.2 Statistical modelling of shape of the femur geometry

The results in Figure 23 show the variation captured per principle mode and the total variation captured in percentage. The first 5 modes captured about 93% of the variation in the training set. This means that these modes account for most of the variance in the observed variables.
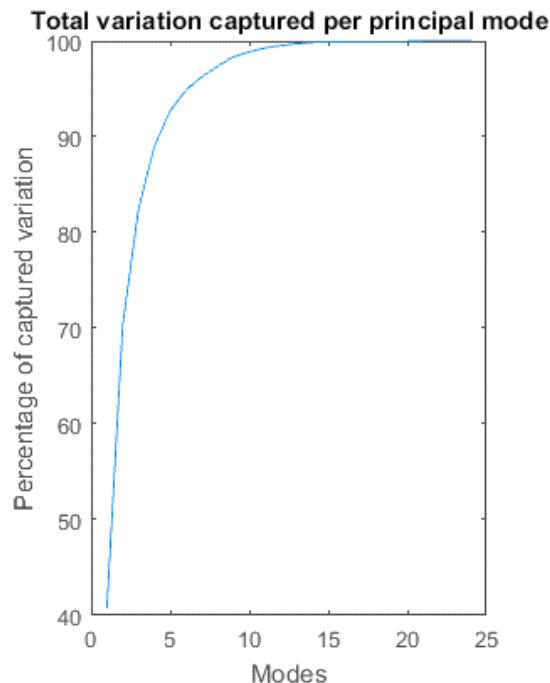
Figure 24: Total variation captured

For a visual understanding of how the first three modes would have looked like, if first three modes were varied using a ± 2 standard deviation, please refer to Figure 16. The physical effect on shape of the femur as stated in the literature paper by Bryan et al. is that the first mode would have captured the scaling effects of the femur with decrease in the femur head radius, the second mode would have captured the increase in femoral shaft width, head radius and length between the head and lesser trochanter. Lastly the third mode would have captured the change in femoral head radius and decrease in condylar size.

3.2 Discussion, limitation, future work and conclusion

All in all, a femur plays a vital role in skeletal system as a weight bearer. For this reason, understanding femoral strain would enable preventative methods that can improve bone quality and decrease fractures of the femur especially for the most affected group which are woman with menopause. Thus the purpose of this study was to firstly identify how strains and activities are correlated and secondly to determine the geometrical variations that are possible within the human femur. The study reported on multiple regression and principal component analysis dataset of 22 Caucasian female subjects' whilst they performed daily activities. Multiple regression was used to predict the correlations between activities and strains whereas PCA was

used to determine the variations of geometry of women aged between 60-77 years old. The results obtained with regards to the influence of activities on strain are exceptional, they indicate that daily activities like normal walking, jumping, standing up and sitting on a chair, going up and down the stairs does play a vital role in the distribution of strain across subjects. The results have shown that there is a very strong correlation, $R^2=0.91$ meaning that activities explain 91% of strain variance in the femur across subjects. Thus the remaining 9% may be attributed to geometry and material bone properties. On the other hand, the variations that are possible within geometry of the femur are 93% which can be explained with the first 5 modes. The first mode captured the effect on shape of the femur, the second mode captured thickening of the bone and the third mode captured an increase in femoral head diameter as shown in Figure 16. This project has begun in the right direction however there is a need for a deeper understanding of the relationship between strains and movement and combining that with geometry to provide a clear understanding on how they have an overall impact on strain variance in the femur. Thus the results obtained in this project would need further validation. This study does not address how material properties makeup part of the 3 parameter when it comes to strain distribution. Yet, it does not negate the overall conclusion that strain distribution is determined by geometry, material properties and loads. The project results just highlight the need for future studies to better quantify femoral strains with regards to activity. A limitation of this project is that not all the subjects analysed had 6 datasets of daily activities, therefore fewer subjects were used to analyse the relationship between strain and activity. Another limitation is that material property distribution of bone was not included in this project as this would have had an impact on the calculation of strain. In the future, it is proposed that to account for that some other parameter would need to be added which is density that would account for the scaling factor and would provide an understanding of how much bone there is. Future works would be to incorporate multiple regression analysis and principal component analysis of geometry and material properties to determine the relationship between activities and bone stiffness in relation to strain. Moreover, future studies will aim to determine how simplified information has an impact on strain. Thus the aim of this project was to create a link between geometry and loads as attributing factors of the distribution of femoral strains. This project has provided a great starting point in that strain distribution in the femur is majorly contributed by the activities a subject is undertaking with a small proportion being contributed by geometry and material bone properties. As the PCA variation has shown that there is a good variation in geometry of the femurs and the multiple regression has demonstrated that there is a positive link between the strains in the bone and daily activities. In conclusion the aim is that the results of this study would serve as a basis for an improved understanding of the relationship between the femur geometry and loads when it comes to strain distribution; and as well as a foundation for the design of anti-osteoporosis intervention for postmenopausal women.

REFERENCES

1. Watts, J.J., J. Abimanyi-Ochom, and K.M. Sanders, *Osteoporosis costing all Australians: a new burden of disease analysis–2012 to 2022.* 2013.
2. Wirth, A., R. Müller, and G. van Lenthe, *Computational analyses of small endosseous implants in osteoporotic bone.* Eur Cells Mater, 2010. **20**: p. 58-71.
3. Dick, C., et al. *Computational Steering for Patient-Specific Implant Planning in Orthopedics*. in *VCBM*. 2008.
4. Prendergast, P., et al., *Computer simulating a clinical trial of a load-bearing implant: an example of an intramedullary prosthesis.* Journal of the mechanical behavior of biomedical materials, 2011. **4**(8): p. 1880-1887.
5. Guerado, E., et al., *Bone mineral density aspects in the femoral neck of hip fracture patients.* Injury, 2016. **47**: p. S21-S24.
6. Martens, M., et al., *The mechanical characteristics of the long bones of the lower extremity in torsional loading.* Journal of biomechanics, 1980. **13**(8): p. 667-676.
7. Currey, J.D., *The mechanical properties of bone.* Clinical Orthopaedics and Related Research, 1970. **73**: p. 210-231.
8. Downey, P.A. and M.I. Siegel, *Bone biology and the clinical implications for osteoporosis.* Physical therapy, 2006. **86**(1): p. 77-91.
9. South-Paul, J.E., *Osteoporosis: part I. Evaluation and assessment.* American family physician, 2001. **63**(5): p. 897-904, 908.
10. Raisz, L.G. and G.A. Rodan, *Pathogenesis of osteoporosis.* Endocrinology and Metabolism Clinics, 2003. **32**(1): p. 15-24.
11. Kaptoge, S., et al., *Prediction of incident hip fracture risk by femur geometry variables measured by hip structural analysis in the study of osteoporotic fractures.* Journal of Bone and Mineral Research, 2008. **23**(12): p. 1892-1904.
12. Föger-Samwald, U., et al., *Molecular mechanisms of osteoporotic hip fractures in elderly women.* Experimental gerontology, 2016. **73**: p. 49-58.
13. Orimo, H., et al., *Diagnostic criteria for primary osteoporosis: year*

2000 revision. Journal of bone and mineral metabolism, 2001. **19**(5): p. 331-337.

14. Carballido-Gamio, J., et al., *Structural patterns of the proximal femur in relation to age and hip fracture risk in women.* Bone, 2013. **57**(1): p. 290-299.

15. Ito, M., et al., *Analysis of hip geometry by clinical CT for the assessment of hip fracture risk in elderly Japanese women.* Bone, 2010. **46**(2): p. 453-457.

16. Takada, J., et al., *Structural trends in the aging proximal femur in Japanese postmenopausal women.* Bone, 2007. **41**(1): p. 97-102.

17. Edwards, W.B., R.H. Miller, and T.R. Derrick, *Femoral strain during walking predicted with muscle forces from static and dynamic optimization.* Journal of biomechanics, 2016. **49**(7): p. 1206-1213.

18. Liebl, H., et al., *In-vivo assessment of femoral bone strength using Finite Element Analysis (FEA) based on routine MDCT imaging: a preliminary study on patients with vertebral fractures.* PloS one, 2015. **10**(2): p. e0116907.

19. Pottecher, P., et al., *Prediction of Hip Failure Load: In Vitro Study of 80 Femurs Using Three Imaging Methods and Finite Element Models—The European Fracture Study (EFFECT).* Radiology, 2016: p. 142796.

20. Cristofolini, L., E. Varini, and M. Viceconti, *In-vitro method for assessing femoral implant—bone micromotions in resurfacing hip implants under different loading conditions.* Proceedings of the Institution of Mechanical Engineers, Part H: Journal of Engineering in Medicine, 2007. **221**(8): p. 943-950.

21. Yosibash, Z., et al., *A CT-based high-order finite element analysis of the human proximal femur compared to in-vitro experiments.* Journal of biomechanical engineering, 2007. **129**(3): p. 297-309.

22. Njeh, C., et al., *Prediction of human femoral bone strength using ultrasound velocity and BMD: an in vitro study.* Osteoporosis international, 1997. **7**(5): p. 471-477.

23. Lotz, J., E. Cheal, and W.C. Hayes, *Fracture prediction for the proximal femur using finite element models: part I—linear analysis.* Journal of biomechanical engineering, 1991. **113**(4): p. 353-360.

24. Lotz, J., E. Cheal, and W.C. Hayes, *Fracture prediction for the proximal femur using finite element models: part II—nonlinear*

analysis. Journal of biomechanical engineering, 1991. **113**(4): p. 361-365.

25. Oh, I. and W.H. Harris, *Proximal strain distribution in the loaded femur. An in vitro comparison of the distributions in the intact femur and after insertion of different hip-replacement femoral components.* J Bone Joint Surg Am, 1978. **60**(1): p. 75-85.

26. Rho, J., M. Hobatho, and R. Ashman, *Relations of mechanical properties to density and CT numbers in human bone.* Medical engineering & physics, 1995. **17**(5): p. 347-355.

27. Currey, J. and G. Butler, *The mechanical properties of bone tissue in children.* J Bone Joint Surg Am, 1975. **57**(6): p. 810-814.

28. Tyrer, J., C. Heras-Palou, and T. Slater, *Three-dimensional human femoral strain analysis using ESPI.* Optics and lasers in engineering, 1995. **23**(5): p. 291-303.

29. Anderson, D.E. and M.L. Madigan, *Effects of age-related differences in femoral loading and bone mineral density on strains in the proximal femur during controlled walking.* Journal of applied biomechanics, 2013. **29**(5): p. 505.

30. Jonkers, I., et al., *Relation between subject-specific hip joint loading, stress distribution in the proximal femur and bone mineral density changes after total hip replacement.* Journal of biomechanics, 2008. **41**(16): p. 3405-3413.

31. Bessho, M., et al., *Prediction of strength and strain of the proximal femur by a CT-based finite element method.* Journal of biomechanics, 2007. **40**(8): p. 1745-1753.

32. Schileo, E., et al., *Subject-specific finite element models can accurately predict strain levels in long bones.* Journal of Biomechanics, 2007. **40**(13): p. 2982-2989.

33. Duda, G.N., E. Schneider, and E.Y. Chao, *Internal forces and moments in the femur during walking.* Journal of biomechanics, 1997. **30**(9): p. 933-941.

34. Duda, G.N., et al., *Influence of muscle forces on femoral strain distribution.* Journal of biomechanics, 1998. **31**(9): p. 841-846.

35. Koivumäki, J.E., et al., *Does femoral strain distribution coincide with the occurrence of cervical versus trochanteric hip fractures? An experimental finite element study.* Medical & biological engineering & computing, 2010. **48**(7): p. 711-717.

36. Schulte, F.A., et al., *Strain-adaptive in silico modeling of bone adaptation—a computer simulation validated by in vivo micro-computed tomography data.* Bone, 2013. **52**(1): p. 485-492.

37. Antibodies, N.R.C.C.o.M.o.P.M., *Summary of Advantages and Disadvantages of In Vitro and In Vivo Methods.* 1999.

38. Taddei, F., et al., *Subject-specific finite element models of long bones: An in vitro evaluation of the overall accuracy.* Journal of Biomechanics, 2006. **39**(13): p. 2457-2467.

39. Cristofolini, L., et al., *In vitro replication of spontaneous fractures of the proximal human femur.* Journal of Biomechanics, 2007. **40**(13): p. 2837-2845.

40. Cristofolini, L., et al., *Mechanical testing of bones: the positive synergy of finite–element models and in vitro experiments.* Philosophical Transactions of the Royal Society of London A: Mathematical, Physical and Engineering Sciences, 2010. **368**(1920): p. 2725-2763.

41. Taddei, F., et al., *Subject-specific finite element models of long bones: an in vitro evaluation of the overall accuracy.* Journal of biomechanics, 2006. **39**(13): p. 2457-2467.

42. Martelli, S., P. Pivonka, and P.R. Ebeling, *Femoral shaft strains during daily activities: implications for atypical femoral fractures.* Clinical Biomechanics, 2014. **29**(8): p. 869-876.

43. Marks, R., et al., *Hip fractures among the elderly: causes, consequences and control.* Ageing research reviews, 2003. **2**(1): p. 57-93.

44. Kobayashi, S., et al., *Poor bone quality or hip structure as risk factors affecting survival of total-hip arthroplasty.* The Lancet, 2000. **355**(9214): p. 1499-1504.

45. Taylor, M., R. Bryan, and F. Galloway, *Accounting for patient variability in finite element analysis of the intact and implanted hip and knee: a review.* International journal for numerical methods in biomedical engineering, 2013. **29**(2): p. 273-292.

46. Byrne, D.P., K.J. Mulhall, and J.F. Baker, *Anatomy & biomechanics of the hip.* The open sports medicine journal, 2010. **4**(1).

47. Norkin, C.C. and D.J. White, *Measurement of joint motion: a guide to goniometry*. 2009: FA Davis.

48. Hughes, P.E., J.C. Hsu, and M.J. Matava, *Hip anatomy and*

biomechanics in the athlete. Sports medicine and arthroscopy review, 2002. **10**(2): p. 103-114.

49.   Drake, R., W. Vogl, and A. Mitchell, *Gray's Anatomy.* Athens: Paschalidis Medical Edition, 2005.

50.   Levangie, P.K. and C.C. Norkin, *Joint structure and function: a comprehensive analysis*. 2011: FA Davis.

51.   Klets, O., *Subject-specific musculoskeletal modeling of the lower extremities in persons with unilateral cerebral palsy.* 2011.

52.   Knudson, D., *Fundamentals of biomechanics*. 2007: Springer Science & Business Media.

53.   Gray, H., *Anatomy of the human body*. 1918: Lea & Febiger.

54.   Keller, T.S. and D.M. Spengler, *Regulation of bone stress and strain in the immature and mature rat femur.* Journal of biomechanics, 1989. **22**(11): p. 1115-1127.

55.   Hamill, J., *Bases biomecânicas do movimento humano.* 1999.

56.   Matheson, G., et al., *Stress fractures in athletes A study of 320 cases.* The American Journal of Sports Medicine, 1987. **15**(1): p. 46-58.

57.   Egan, J.M., *A constitutive model for the mechanical behaviour of soft connective tissues.* Journal of biomechanics, 1987. **20**(7): p. 681-692.

58.   Bankoff, A.D.P., *Morfologia e cinesiologia: aplicada ao movimento humano*. 2007: Guanabara Koogan.

59.   Bankoff, A.D.P., *Biomechanical characteristics of the bone*. 2012: INTECH Open Access Publisher.

60.   Keaveny, T.M. and W.C. Hayes, *Mechanical properties of cortical and trabecular bone.* Bone, 1993. **7**: p. 285-344.

61.   Voo, L., M. Armand, and M. Kleinberger, *Stress fracture risk analysis of the human femur based on computational biomechanics.* Johns Hopkins APL Tech Dig, 2004. **25**(3): p. 223-30.

62.   Rho, J.-Y., L. Kuhn-Spearing, and P. Zioupos, *Mechanical properties and the hierarchical structure of bone.* Medical engineering & physics, 1998. **20**(2): p. 92-102.

63.   Henkel, J., et al., *Bone regeneration based on tissue engineering conceptions—a 21st century perspective.* Bone research, 2013. **1**(3): p. 216.

64.   Sarkalkan, N., et al., *Statistical shape and appearance models for*

fast and automated estimation of proximal femur fracture load using 2D finite element models. Journal of biomechanics, 2014. **47**(12): p. 3107-3114.

65. Goldman, L.W., *Principles of CT and CT technology.* Journal of nuclear medicine technology, 2007. **35**(3): p. 115-128.

66. Imai, K., *Computed tomography-based finite element analysis to assess fracture risk and osteoporosis treatment.* World journal of experimental medicine, 2015. **5**(3): p. 182.

67. Couteau, B., Y. Payan, and S. Lavallée, *The mesh-matching algorithm: an automatic 3D mesh generator for finite element structures.* Journal of biomechanics, 2000. **33**(8): p. 1005-1009.

68. Keyak, J.H. and S.A. Rossi, *Prediction of femoral fracture load using finite element models: an examination of stress-and strain-based failure theories.* Journal of biomechanics, 2000. **33**(2): p. 209-214.

69. Bessho, M., et al., *Prediction of the strength and fracture location of the femoral neck by CT-based finite-element method: a preliminary study on patients with hip fracture.* Journal of Orthopaedic science, 2004. **9**(6): p. 545-550.

70. Taddei, F., et al., *Finite-element modeling of bones from CT data: sensitivity to geometry and material uncertainties.* IEEE transactions on biomedical engineering, 2006. **53**(11): p. 2194-2200.

71. Keyak, J., I. Lee, and H. Skinner, *Correlations between orthogonal mechanical properties and density of trabecular bone: use of different densitometric measures.* Journal of biomedical materials research, 1994. **28**(11): p. 1329-1336.

72. Parashar, S.K. and J.K. Sharma, *A review on application of finite element modelling in bone biomechanics.* Perspectives in Science, 2016. **8**: p. 696-698.

73. Huiskes, R. and E. Chao, *A survey of finite element analysis in orthopedic biomechanics: the first decade.* Journal of biomechanics, 1983. **16**(6): p. 385-409.

74. Verhulp, E., B. van Rietbergen, and R. Huiskes, *Load distribution in the healthy and osteoporotic human proximal femur during a fall to the side.* Bone, 2008. **42**(1): p. 30-35.

75. Nikishkov, G., *Introduction to the finite element method.* University of Aizu, 2004.

76. Martelli, S., et al., *Strain energy in the femoral neck during exercise.* Journal of biomechanics, 2014. **47**(8): p. 1784-1791.

77. Martelli, S., M.E. Kersh, and M.G. Pandy, *Sensitivity of femoral strain calculations to anatomical scaling errors in musculoskeletal models of movement.* Journal of biomechanics, 2015. **48**(13): p. 3606-3615.

78. Rasmussen, J., et al. *Musculoskeletal modeling as an ergonomic design method.* in *International Ergonomics Association XVth Triennial Conference.* 2003.

79. Arnold, A.S., S.S. Blemker, and S.L. Delp, *Evaluation of a deformable musculoskeletal model for estimating muscle–tendon lengths during crouch gait.* Annals of biomedical engineering, 2001. **29**(3): p. 263-274.

80. Blemker, S.S., et al., *Image-based musculoskeletal modeling: Applications, advances, and future opportunities.* Journal of magnetic resonance imaging, 2007. **25**(2): p. 441-451.

81. Davis, R.B., et al., *A gait analysis data collection and reduction technique.* Human movement science, 1991. **10**(5): p. 575-587.

82. Dorn, T.W., A.G. Schache, and M.G. Pandy, *Muscular strategy shift in human running: dependence of running speed on hip and ankle muscle performance.* Journal of Experimental Biology, 2012. **215**(11): p. 1944-1956.

83. Rosipal, R. and N. Krämer, *Overview and recent advances in partial least squares*, in *Subspace, latent structure and feature selection.* 2006, Springer. p. 34-51.

84. Stolzenberg, R.M., *Multiple regression analysis.* Handbook of data analysis, 2004: p. 165-208.

85. Mei, L., et al. *Statistical shape modelling: how many modes should be retained?* in *Computer Vision and Pattern Recognition Workshops, 2008. CVPRW'08. IEEE Computer Society Conference on.* 2008. IEEE.

86. Bryan, R., P.B. Nair, and M. Taylor, *Use of a statistical model of the whole femur in a large scale, multi-model study of femoral neck fracture risk.* Journal of biomechanics, 2009. **42**(13): p. 2171-2176.

87. Bryan, R., et al., *Statistical modelling of the whole human femur incorporating geometric and material properties.* Medical engineering & physics, 2010. **32**(1): p. 57-65.

88. Cootes, T.F. and C.J. Taylor. *Statistical models of appearance for medical image analysis and computer vision*. in *Medical Imaging 2001*. 2001. International Society for Optics and Photonics.

89. Cootes, T.F., et al., *Active shape models-their training and application.* Computer vision and image understanding, 1995. **61**(1): p. 38-59.

90. Cootes, T.F., G.J. Edwards, and C.J. Taylor. *Comparing Active Shape Models with Active Appearance Models*. in *BMVC*. 1999. Citeseer.

91. Castro-Mateos, I., et al., *Statistical Shape and Appearance Models in Osteoporosis.* Current osteoporosis reports, 2014. **12**(2): p. 163-173.

92. Daruwalla, Z.J., et al., *An application of principal component analysis to the clavicle and clavicle fixation devices.* Journal of orthopaedic surgery and research, 2010. **5**(1): p. 1.

93. Brodziak-Dopierała, B., et al., *The application of principal component analysis to interpretation of occurrence of metals in the femur head.* Polish Journal of Environmental Studies, 2010. **19**(1): p. 49-58.

94. Jolliffe, I., *Principal component analysis*. 2002: Wiley Online Library.

95. Flury, B. and H. Riedwyl, *Multivariate Statistics: A Practical Approach*. JSTOR.

96. Matlab, S., *What is MATLAB?* The MathWorks, Natick, MA, 2012.

APPENDIX

Matlab codes
The Matlab codes used in generation of PCA

```
[F, V2, C] = rndread([dir,'FXMP01_femur_r.stl']); % read stl
iteration_limit=5;
converge_tolerance=10;
visualise=1;
verbose=1;
F= importdata ('D:\Test\geometry\results\one.txt');
[femlength_func femlength_max femlength_bicond AP_dist_dim ML_dist_dim, ...
    AP_prox_dim ML_prox_dim ps_m2_area ps_m2_rad_major ps_m2_rad_minor, ...
    ps_m4_area ps_m4_rad_major ps_m4_rad_minor ps_m6_area ps_m6_rad_major, ...
    ps_m6_rad_minor ps_m8_area ps_m8_rad_major ps_m8_rad_minor headrad, ...
    hrad_major hrad_minor neck_isth_maj_rad neck_isth_min_rad fem_neck_length,
    fem_ante_ang fem_ccd_angle head_centre pp2 ps2 mp2] = Register_FCS4(F, ...
    downsample, iteration_limit, converge_tolerance, visualise, verbose);

TRIALS = 28; % # number of patients
NODES = 25; % length of the matrix

% The covariance based PCA:

X_mean = mean(X);
X_std = std(X, 0, 1);

for i= 1 : TRIALS
    X_z(i,1:NODES) = X(i,1:NODES) - X_mean(1:NODES);
end
[U,S,V] = svd(X_z,'econ'); % This is the PCA part! note: using the 'economy' setting reduces
output size

Eig_Val = diag(S);  % Get just the diagonal elements of the 2D matrix S (i.e. S(i,j) where i == j) -
this is a 1D vector
Eig_Vec = V';       % Identify Eigenvalues and Eigenvectors
E = (Eig_Val).^2;   % Square Eigenvalues to find energy terms

% Create plot of energy in eigenmodes
Energy_Total = sum(E);
Energy_per_decay = 100 * E / Energy_Total;
Energy_per_total = cumsum(Energy_per_decay);

 figure(1); plot(Energy_per_decay); title('"Energy" per Principal Component Term')
 ylabel('Energy');
 xlabel('principal component');
 figure(2); plot(Energy_per_total); title('Cumulative "Energy" per Principal Component Term')
 ylabel('Energy');
 xlabel('principal component');
```

The Matlab codes used in for multiple regression Analysis
```
%% backup on turbo
clear all; clc
simulations; % load the simulations names
dirm = 'D:\Raissa/';
```

```matlab
dirb = 'D:\Test\';
ss = size(sim.subject);
matr = [];
tic
eln = [];
md = 1; %scaled generic
for subject = 2 % relates to subject number
    st = size(sim.subject{subject}.task);
    for task = 6 %st(2); relates to task; this enables you to move from one task folder to another;
(what was originally there (2:6))
        %% LOAD THE JOINT MOMENTS
        model = sim.subject{subject}.model{md};
        dir1
=[dirm,sim.subject{subject}.name{1},'\SCALED_MODEL\',sim.subject{subject}.task{task},'\'];    %
picking things from the directory
        dir2
=[dirb,sim.subject{subject}.name{1},'\SCALED_MODEL\',sim.subject{subject}.task{task},'\'];    %
where your saving the things to which directory
        id_file = [sim.subject{subject}.name{1},'_',...
            model,'_',...
            sim.subject{subject}.task{task},'_inverse_dynamics']; % contains moments at the hip,
knee and ankle
        if exist([dir1,'inverse_dynamics\',id_file,'.sto'],'file') == 2
            x = importdata([dir1,'inverse_dynamics\',id_file,'.sto'],'\t',7); % 7 relates to you being able
to see the whole inverse file
            if sim.subject{subject}.side == 0
                col = 8:12; % right femur
                x = x.data(sim.subject{subject}.frames{task},col);
            else
                col = 15:19; % left femur
                x = x.data(sim.subject{subject}.frames{task},col);
            end
        end

        %% strain
        matr =[];
        elem_list =[]; k = 1;
        sx = size(x);
        ycalc = []; Pe = []; yy= [];
        for bonr = 1:32 % iterates bone regions all 32
            inp_file   =   [sim.subject{subject}.name{1},'_SCALED_',sim.subject{subject}.task{task}];
%input file is the proper mesh for the FE model
            if exist([dir1,sim.subject{subject}.name{1},...
                    '_SCALED_',sim.subject{subject}.task{task},'_PROCESSEDRESULTS.mat'],'file')
== 2 % contains strains
                s = load([dir1,sim.subject{subject}.name{1},...
                    '_SCALED_',sim.subject{subject}.task{task},'_PROCESSEDRESULTS.mat']);
                % 7 relates to you being able to see the whole inverse file
            end
            for frame = 1:sx(1) % runs all the frames in the tasks
                sbonr = size(s.out{bonr}.values); %
                tmp =[];
                y = NaN(sbonr(3),sbonr(1)); % 1 is the number of elements in the first place
                for eln = 1:floor(sbonr(1)/100):sbonr(1) % eln means element number (creating a matrix
of elements where the strain if each element is)
                    y = s.out{bonr}.values(eln,2,:); % y is a colume vector (produces strain per element)
                    y = y(:)*1e6; % declares the size of y * 24 the size
```

```matlab
            en = s.out{bonr}.values(eln,1,frame); % en means element number
            %%% regression (does it automatically)
            matr(en,1:6,frame) = ([ones(size(x,1),1),x]\y)';
            elem_list(k) = en; k = k+1;
            yy(en,:)=y'; % meant to increase the dimension of y
            ycalc(en,:)= ([ones(size(x,1),1),x]* (matr(en,1:6,frame))')';
            Pe(en,:)= max (abs(y- ycalc(en,:)')); % how to get the peak value
            RMSE (en,:)= sqrt(mean((yy(:) - ycalc(:)).^2));

        end

      end
    end
  end

end

toc
```